Exosomes from Gastric Cancer Suppressed Adipo-differentiation of Adipose Mesenchymal Stem Cells to Promote Cancer-associated Cachexia via miR-155/ C/EPBβ pathway

Ying Liu (yingliu0109@163.com)
Tianjin tumor hospital
Dan Lin
Tianjin Tumor Hospital
Huiya Wang
Tianjin Tumor Hospital
Haiyang Zhang
Tianjin Tumor Hospital
Ting Deng
Tianjin Tumor Hospital
Rui Liu
Tianjin Tumor Hospital
Tao Ning
Tianjin Tumor Hospital
Ming Bai
Tianjin Tumor Hospital
Guoguang Ying
Tianjin Tumor Hospital
Yi Ba
Tianjin Tumor Hospital

Research

Keywords: exosomes, adipose mesenchymal stem cells, miR-155, cachexia, gastric cancer

Posted Date: November 12th, 2020

DOI: https://doi.org/10.21203/rs.3.rs-103656/v1

Abstract

BACKGROUND: Cancer-associated cachexia (CAC) is defined as a multifactorial syndrome including depletion of adipose tissue and skeletal muscle. Adipose tissue wasting, as a key characteristic of CAC, occurs early and is related with poor survival. However, the influence of exosomes on adipo-differentiation in CAC remained be mysterious.

METHODS: Oil-red staining, western blotting, and real-time polymerase chain reaction (RT-PCR) were used to investigate the adipo-differentiation capacity of A-MSCs from GC patients and healthy donors. Adipo-differentiation capacity of A-MSCs treated with exosomes from GES-1 or GC cell lines was also detected. To further explore the effects of exosomal miR-155 on adipo-differentiation in vitro, we carried out luciferase reporter assay. Finally, to evaluate the function of exosomal miR-155 in vivo, BALB/c mice were subcutaneously transplanted with SGC7901 cells transfected with lentivirus containing a miR-155 overexpressing (miR-155 OE) sequence or miR-155 shRNA (miR-155 KO) or control lentivirus(NC) to observe the change of adipo-differentiation of A-MSCs.

RESULTS: We showed that miR-155 was high expressed in adipose mesenchymal stem cells (A-MSCs) isolated from GC patients, which exhibited significantly suppressed adipo-differentiation. Mechanistically, targeting C/EPBβ and suppressing C/EPBα and PPARγ by GC exosomal miR-155 was demonstrated to be involved in impairing the differentiation of A-MSCs into adipocytes. The expression of C/EPBβ C/EPBα and PPARγ were rescued through downregulating miR-155 in GC exosomes. Moreover, overexpression of miR-155 improved cancer cachexia in tumor-implanted mice, charactered by weight loss, tumor progression and low expression of C/EPBβ, C/EPBα, and PPARγ in A-MSCs as well as FABP4 in tumor-related adipose tissue. Decreasing level of miR-155 in implanted tumor blocked the anti-adipogenic effects of GC.

CONCLUSION: GC exosomsal miR-155 suppressed adipo-differentiation of A-MSCs via targeting C/EPBβ of A-MSCs plays a crucial role in CAC.

Introduction

Cancer-associated cachexia (CAC), a metabolic disorder characterized by progressive loss of body fat and skeletal muscle wasting[1]. It is a common occurrence in gastric cancer which leading 20% of cancer-related death[2]. Recent researches and clinical trials on therapy for CAC have focused on the changes in adipose tissue, especially increased lipolysis in CAC[3, 4]. However, limitation of research nowadays is whether adipogenesis have effects on CAC. More detailed comparative studies on adipogenesis, which is identified as a key hallmark of remaining balance with lipolysis will be much-needed.

Adipocytes are devoloped from A-MSCs that have the capacity of multipotent adult stem cells to different into several cell type[5]. Thus, further understanding change of molecular mechanisms of adipogenesis of A-MSCs in cancer is very crucial for the development of novel strategies to treatment of CAC. The renewing of adipocyte relies on orchestrated activation of transcription factors, inducing differentiation of

A-MSCs to mature adipocytes[6, 7]. So A-MSCs is a perfect cell model to study adipogenesis at a level of stem cells. Members of the CCAAT/enhancer-binding protein (C/EBP) family and the preceding peroxisoe proliferator-activated receptors (PPARs) family are the two most critical transcription factors associated to adipogenic-specific program, among which C/EPBβ plays an essential role[8–10]. During A-MSCs adipo-differentiation, activated C/EBPβ triggers transcription of C/EPBα and PPARγ, which in turn coordinately activate genes, such as fatty acid-binding proteins (FABPs), fatty acid transport proteins (FATPs), whose expression produces for terminal adipocyte[11, 12].

Exosomes are microvesicles with diameters of 40–100 nm that are released by most cell types[13]. An increasing number of studies have shown that exosomes play an importance role in intercellular communication, because it contains a variety of RNAs, proteins and lipids, especially, microRNAs have recently been identified as a naturally occurring class of endogenous noncoding RNAs[14]. A recent article published in Nature Reviews demonstrated that extracellular vesicles packing cargo reach subpopulations of muscle cells and mediate cachexia. While the effects of GC exosomes on adipogenesis have not been elucidated[15].

In the current study, we detected miR-155 is upregulated in the plasma and A-MSCs of GC patients, which was negetively correlated with adipogenesis level of A-MSCs GC patients. Additionally, study in vitro demonstrated that the inhibition of adipogenesis in A-MSCs was caused by exosomal miR-155secreted from GC cells.What's more, our further investigation revealed miR-155 can directly target the 3'UTR of C/EPBβ which finally bolcked the C/EPBα and PPARγ. In vivo, by analyzing the levels of C/EPBβ C/EPBα and PPARγ in MSCs from mice inguinal adipose tissues (mA-MSCs), as well as FABP4 expression in adipose tissues of mice, we concluded that the knockdown of miR-155 in cancer cells significantly rescues the adipogenesis impairment of A-MSCs caused by GC. Herein, the specific targeting of exosomal miR-155 from GC on C/EPBβ is confirmed to be involved in the inhibitive effects of GC on A-MSCs adipogenesis.

Methods

Cell culture

Adipose tissues were respectively obtained from patients undergoing liposuction and GC patients peritoneam and healthy donors according to procedures approved by the Ethics Committee of Tianjin Medical University Cancer Institute and Hospital. A-MSCs were isolated and culture-expanded as previously discribed[16]. The cells were incubated in DMEM/F-12 (Gibco,USA) supplemented with 10% FBS (Gibco,USA), 1% penicillin and streptomycin (Solarbio, China), 2 mmol/L glutamine and 10 ng/mL epidermal growth factor (PeproTech). A-MSCs at passage 3-5 were choosed for the folowing research. To inducing A-MSCs-adipogenesis, A-MSCs were remaining under adipogenic differentiation medium. (DMEM/F-12 1μM dexamethasone, 0.5 mM 3-isobutyl-1-methylxanthine, 0.5 μg/ml insulin, 0.5 mM isobutylmethylxanthine) with 10% FBS.

SGC7901, MGC803 (human gastric adenocarcinoma cell) were bought from cell bank of Chinese Academy of Sciences (Shanghai, China). SGC7901 and MGC803 cells were cultured in DMEM medium (Gibco, USA) supplemented with 10% FBS

exosomes isolation and identification

Exosomes in medium was isolated according to previous report. GC cells culture media were collected at 300g and 3,000g eliminate cells and debris. Next, the supernatant was centrifuged at 100000g for 70 min at 4℃ to abtain exosomes. Exosomes was dropped onto the copper grid and negatively stained with 3% (w/V) sodium phosphotungstate solution (pH6.8) for 5 min and washed gently with double distilled water. Exosomes were observed and photographed by transmission electron microscopy (TEM). Western Blot was used to detected exosomes specific markers, including Alix, Tgs101 and CD63. selected randomly to measure the mean diameterusing the Nanosight NS 300 system (NanoSight technology, Malvern, UK).

RNA isolation and quantitative RT-PCR

Total RNA was isolated from the cultured cells, exosomes, and tissues using TRIzol Reagent (Invitrogen), according to the manufacturer's instruction. cDNA was obtained by using avian myeloblastosis virus (AMV) reverse transcriptase (TaKaRa). Quantitis of miR-155 was detected via TaqMan miRNA probes (Applied Biosystems) and normalized to U6 snRNA expression. mRNA expression levels of C/EPBβ, C/EPBα and PPARγ was performed with the SYBR Green PCR Master Mix (Qiagen) through ABI PRISM 7900 (AppliedBiosystems). The mRNA expression was normalized to GADPH. All reactions were performed at least in triplicate. Relative levels of genes were calculated with the 2-ΔCT method. The primer sequences were as follows:

5’GGGCCCTGAATCGCTTA A3’(C/EPBβ, sense);

5’ATCAACAGCAACAAGCCCG3’(C/EPBβ, anti-sense);

5’- GAAGTTGGTGGAGCTGTCGG-3’ (C/EPBα, sense);

5’- TGAGGTATGGGTCGTTGGGA-3’ (C/EPBα, anti-sense);

5’- AGCCTCATGAAGAGCCTTCCA-3’ (PPARγ, sense);

5’- ACCCTTGCATAATTCACAAGC-3’ (PPARγ, anti-sense);

5’-AGAAGGCTGGGGCTCATTTG-3’ (GAPDH, sense);

5’-AGGGGCCATCCACAGTCTTC-3’ (GAPDH, anti-sense).

Western blotting

The total protein was extracted using RIPA buffer. The protein concentration was quantified by the BCA Protein Assay kit (Thermo). Protein (30 μg) of each sample was loaded into a 10% sodium dodecyl sulfate polyacrylamide gel electrophoresis gel(SDS-PAGE gels) and transferred onto polyvinylidene fluoride (PVDF) membranes (Millipore). After blocking with 5% BSA at room temperature for 1 h, membranes were incubated with primary antibodies (1/1000 dilution) at 4℃ overnight . After membranes were incubated with corresponding secondary antibodies (1/5000 dilution) for 1 h at room temperature. Blots were detected using enhanced chemiluminescence solution (Invitrogen) and visualized with the ImageQuantLAS-4010 (GE).

Oil red O staining

The cells were washed there times with phosphate-buffered saline (PBS) gentally and then fixed with 10% formaldehyde for 10 min at room temperature. After fixation, cells were treated with filtered 0.25% oil red O solution for 40 minutes. red-stained lipid droplets in cells were observed and photographed by light microscopy.

Luciferase assay

The miRNA target prediction and analysis were performed with the algorithms from TargetScan (http://www.targetscan.org/vert_72/), PicTar(https://pictar.mdc-berlin.de/), and miRanda (http://miranda.org.uk/).

The reporter plasmid p-MIR-C/EPBβ was designed by Genescript (Nanjing, China) containing the predicted miR-155 binding site. Part of the wild-type and mutated 3’-UTR of C/EPBβ was cloned into the firefly luciferase reporter. For the luciferase reporter assays, 2 mg firefly luciferase reporter plasmid; 2 mg b-galactosidase vector; and equal doses(200 pmol) of mimics, inhibitors, or scrambled negative control RNA were transfected into AMSCs. At 24h after transfection, luciferase activity of cells were analysed by using the Dual Luciferase Assay Kit (Promega) according to the manufacturer’s instructions.

Immunofluorescence

Cells were cultured in 12-well plates with slides. At harvest, the cells were first fixed with 4% paraformaldehyde and then permeabilized with 0.2% Triton X-100 for 10 min, followed by confinement for 1 h. Then, the cells were incubated with C/EPBβ, C/EPBα, and PPARγ (1:100; Abcam) at 4 °C overnight and FITC goat anti-rabbit IgG (Invitrogen) for 1h in the dark at RT. DAPI (Solarbio, China) was used for nuclear staining. For confocal microscopy, a Nikon C2 Plus confocal microscope was used.

Immunohistochemistry

The inguinal adipose tissues were fixed in 4% paraformaldehyde, embedded in paraffin, sectioned and then stained with anti-FABP4 antibodies (Abcam). Quantitative analysis was conducted by quantifying the fluorescence intensity from at least five sections.

Establishment of tumor in nude mice

lentiviral expression plasmids that were used to increase or decrease the expression of miR-155 and control lentivirus were purchased from Shanghai Genechem. Puromycin (Sigma-Aldrich, USA) was used to successfully obtain stably infected SGC7901 cells. Cells infected with lentivirus above were injected into nude mice by orthotopic implantation. Mice were sacrificed and tumors were removed at the 28th Day.

Statistics

All experiments were performed in triplicate, and the results are presented as the mean value ± standard deviation. The data were statistically analyzed using Student's

t-test in SPSS statistical software, with $p < 0.05$ considered statistically significant. *

indicates $p< 0.05$; ** indicates $p< 0.01$ and *** indicates $p<0.001$

Results

Adipo-differentiation of A-MSCs from GC Patients Is inhibited and Negatively Correlated with miR-155

We initially analysed GC patients survival through a tumor database (http://kmplot.com) revealed that high miR-155 expression level is a poor prognostic factor in GC patients (Fig. 1A). Then, the level of miR-155 in serum of GC patients and healthy donors was measured. A high level of miR-155 expression was present in serum of GC patients (Fig. 1B). Then we also detected the capacity of adipo-differentiation in A-MSC isolated from peritoneum adipose tissue of GC patients (GC group), and A-MSC from subcutaneous adipose tissue of healthy donors (HD group) as normol control. Investigated by Oil Red O staining, the accumulation of lipid droplets in A-MSCs isolating from peritoneum of GC patients was decreased (Fig. 1C). As a crucial transcription factor of early adipo-differentiation stage, C/EBPβ was significantly decreased in A-MSCs isolating from GC patients (Fig. 1D-E). We performed RT-PCR to detect the expression level of miR-155 and the results indicated that miR-155 in A-MSC was obviously increased in the GC group compared to HD group (Fig. 1F). In conclusion, the results above suggested that miR-155 can promote GC progression and negatively correlated with adipogenesis capacity of A-MSCs.

Identification And Characterization Of A-mscs And Gc Exosomes

The morphology of A-MSCs present like fibroblasts (Fig. 2A) and the lipid drops formation was observed after culturing in adipogenic differentiation medium (Fig. 2B-C). A-MSCs were positive for CD44, CD73, CD90, CD105, CD166 and HLA-ABC, but negative for CD31, CD133, CD14, CD34, CD45 and HLA-DR

(Fig. 1D). In our preliminary experiment, TEM showed that SGC7901-exosomes exhibited a round-shaped morphology (Fig. 1E) with a size ranging from 50 to 100 nm (Fig. 1G). In addition, Tgs101 and CD63 were highly expressed by SGC7901 exosomes and MGC803 exosomes (Fig. 1F). Exosomes stained with PKH26 were added into the medium of A-MSCs, the phagocytosis was recorded at 2 h, 4 h and 6 h after co-culture through confocal microscopy. It showed that the uptaken of SGC7901 exosomes increases with the time of co-culture and over 80% of the A-MSCs exhibited PKH67 staining although the intensity of the red fluorescence of the positive MSCs (Fig. 1H). Taking together, our results proved that A-MSCs and exosomes with high purity were successfully isolated, as well as SGC7901-exosomes can be taken up by A-MSCs.

Gc Cell Derived Exosomes Inhibited Adipo-differentiation Of A-mscs

Since SGC7901 exosomes and MGC803-exosomes could be taken up by A-MSCs, then we determined whether the adipogenic differentiation of A-MSCs was changed by GC exosomes. A-MSCs were treated with different doses of SGC7901 exosomes and MGC803 exosomes (50ug/ml and 70ug/ml) in adipogenic induction medium for 5 days. GC-exosomes treatment significantly decreased lipid droplets in A-MSCs as the concentration exosomes increased, compared with GES-1-exosomes (50ug/ml) treatment groups (Fig. 3A). GC exosomes treatment, both SGC7901 exosomes and MGC803 exosomes, also decreased mRNA expression levels of adipogenic transcription factors C/EBPβ mRNA, C/EBPα, and PPARγ (Fig. 3B, D). Moreover, the protain expression of C/EBPβ, C/EBPα, and PPARγ in A-MSCs cultured in adipogenic induction medium were inhibited by GC-exosomes (Fig. 3C, E). The results above suggested that GC exosomes acted as a negative regulator in adipo-differentiation of A-MSCs.

Gc-exosomal Mir-155 Tageting C/ebpβ Expression In A-mscs

The miR-155 binding sites in the 3’UTR of C/EBPβ mRNA are shown in Fig. 4A. Transfection of miR-155 mimics markedly reduced luciferase activity, whereas luciferase levels were relatively enhanced by miR-155 inhibitors. However, the inhibitory activity was lost when the binding sites were mutated (Fig. 4B). The data indicated miR-155 suppressed C/EBPβ expression by binding to C/EBPβ 3’UTR in adipocytes. Additionally, to further explore the influence of miR-155 on the adipogenic differentiation of A-MSCs, normal control mimics, miR-155 mimics, normal control inhibitors, and miR-155 inhibitors were directly transfected into A-MSCs. As shown in Figs. 4C and 4D, RT-PCR was used to analyze the level of miR-155 in above groups. Cultured in adipogenic differentiation medium for 5 days later, western blotting was used to assess the expression level of C/EBPβ. The expression of C/EBPβ in A-MSCs were much lower in miR-155 mimics group than that in normal control mimics group, while the expression of C/EBPβ was significantly enhanced in A-MSCs transfected with miR-155 inhibitors compared with normal control inhibitors. However there was no significant change in C/EBPβ mRNA (Fig. 4E-G). Moreover, we also

found that miR-155 was highly expressed in exosomes derived from SGC7901 cells and MGC803 cells (Fig. S-A). To verify the function of miR-155 in GC-exosomes, SGC7901 cells were relatively transfected with miR-155 inhibitors or normal control inhibitors, then isolating exosomes of each group (SGC exosomes In.miR-155 or SGC exosomes In.NC) and co-cultured with A-MSCs (Fig. 4H). miR-155 level in SGC7901 cells exosomes and A-MSCs treated with SGC exosomes In.miR-155 or SGC exosomes In.NC (100 μg/ml) for 8 h were measured by RT-PCR, and that the level of miR-155 was markedly decreased in SGC exosomes In.miR-155 (Fig. 4I) and A-MSCs treated with that (Fig. 4J). Under adipo-differentiational condition for 5 days, the expression of C/EBPβ, C/EPBα and PPARγ in A-MSCs treated with SGC exosomes In.miR-155 (100 μg/ml) were much higher than those in SGC exosomes In.NC group (Fig. 4L,M). But no significant change of C/EBPβ mRNA in A-MSCs was obvioused in those two groups (Fig. 4K). These results suggested that C/EBPβ was a downstream target gene of miR-155, the upregulation of GC exosomal miR-155 expression may be responsible for the decreased expression level of C/EBPβ, as well as the downstream protein C/EPBα and PPARγ in A-MSCs.

GC Exosomal miR-155 Contributes to The Lose of Adipose Mass in Vivo

To identify whether GC Exosomal miR-155 suppressed adipo-differentiation of A-MSCs and promoted cancer cachexia in vivo, BALB/c mice were subcutaneously injected with SGC7901 cells transfected with lentivirus containing a miR-155 overexpressing (miR-155 OE) sequence or miR-155 shRNA (miR-155 KD) or control lentivirus(NC). Then PBS was used as a negative control (Fig. 5A). 4 weeks later, all of the tumors, plasma and inguinal adipose tissues were harvested. The sizes of tumors and weight of mice were measured during the experiment. Compared with control group, the diameter of tumors was remarkably enhanced in the miR-155-OE group, while in the control group, the growth of tumors was visibly inhibited (Fig. 5B). Similarly, weight of mice was obviously reduced in miR-155 OE group, while which was increased in the miR-155 KD group (Fig. 5C). The tumors obtained were photographed and analyzed (Fig. 5D-E). Images of inguinal adipose tissues from the four groups are shown in Fig. 5F, and the lengths and weights of these adipose tissues in miR-155 OE group were decreased. As expected, the miR-155 KD rescued that trend (Fig. 5G-H). Additionally we detected the expression of fatty acid binding protein-4 (FABP4) in inguinal adipose tissues. A down-regulation of FABP4 was detected in tumor-implanted groups, which shown a negative correlation with miR-155 level (Fig. 5I). The data above demonstrated that GC-exosomes carried miR-155 can be delivered into adipose tissue and lead to decrease of adipose mass which is caused by suppressing C/EBPβ.

GC exosomal miR-155 suppresses A-MSCs adipo-differentiation via targeting C/EBPβ/C/EBPα/PPARγ in vivo

To further investigated the biological role of miR-155 in CAC, initially we detected lipid-formed capacity in mA-MSCs after culturing in adipogenic differentiation medium (Fig. 6A), miR-155 in mA-MSCs and serum esosomes were distinctly upregulated in the miR-155 OE group (Fig. 6B, Figure S-B). The expression of C/EBPβ, C/EBPα and PPARγ in mA-MSCs of each group indicated a negtive relationship with miR-155 level of adipose tissue (Fig. 6C, D). We further investigated the expression of C/EBPβ, C/EBPα and PPARγ

in mA-MSCs adipo-differentiated with adipogenic medium for 5 days. The results a significant decrease of C/EBPβ, C/EBPα, PPARγ expression due to implanted-tumor, especially in miR-155 OE group, but this decrease was rescued when miR-155 was knocked down in implanted-tumor (Fig. 6E). These findings indicated that GC-exosomes carried miR-155 acted as a promotive role on CAC via suppressing of C/EBPβ in A-MSCs..

Discussion

Continuous adipose tissue mass loss could result in devastating outcomes in CAC Patients, which cannot be explained by reduced food intake alone[17]. Patients with CAC often present symptom of emaciation without anorexia and the supplementation of nutrition fails to reverse CAC[18–20]. Numerous deeper mechanistic researches manifested that the lose of adipose tissue preceded skeletal muscle in CAC, nevertheless the underlying mechanisms on depletion of adipose tissue occurred in CAC still remains mysterious. Recent studies implied that the inflammational and immunologic factors such as interleukin-6, tumor growth factor-β increased lipolysis[21, 22]. Furthermore, reseachers focused their attention on white adipose tissue (WAT) browning. Previous work in our laboratory have proved that exosomal ciRS-133 are involved in WAT browning and play a key role in CAC[23]. Adipo-differentiation is a crucial process of formation and renewing of adipocytes. However, little is known about the effect of exosomes on the change of adipo-differentiation in CAC.

In addition, miR-155 has been confirmed as “oncomiR” in virious cancer types, including lymphoma, gastric cancer and breast cancer[24]. More importantly, recent work in our laboratory reported that GC exosomal miR-155 could promote angiogenesis through targeting c-MYB and FOXO3[25, 26]. According to our clinical results, we have confirmed that adipo-differentiation was blocked by upregulating miR-155 in A-MSCs obtained from GC patients. The evidence mentioned above led us to hypothesize that exosomal miR-155 may act as a promoted factor for CAC by attenuating adipo-differentiation of A-MSCs. As expected, miR-155 had repressing effects on adipogenesis of A-MSCs. First, miR-155 was upregulated in serum of GC patients and exosomes devived from GC cell lines. Second, GC exosomes can impair adipogenesis of A-MSCs, but the adipogenesis capibility was recovered as miR-155 knocking down in GC exosomes. Third, when miR-155 was overexpressed in implanted-tumor in vivo, the weight of mice and size of inguinal adipose tissues was dramatically reduced, accomplied with less expression of FABP4 in adipocyte. Therefore, it is necessary to further value the underlying mechanisms of how exosomal miR-155 influenced adipogenesis.

Adipogenesis is a highly controlled process via sequential activation of transcription factors. C/EBPβ is rapidly (< 8 h) expressed under induction of adipo-differentiation[27]. (C/EBPβ-/-) mice fail to undergo mitotic clonal expansion and differentiate into adipocytes[28]. This finding provides further compelling proof that C/EBPβ is indispensable for adipogenesis. Beginning 12 h after the induction of adipo-differentiation, C/EBPβ activated the C/EBPα and PPARγ gene transcriptionally [29]. Subsequently C/EBPα and PPARγ function together to trans-activate the large group of adipogenesis assoxiated gene, such as FATP1, FABP4 and LPL which are essential for the formation of mature adipocytes [30, 31]. In

vitro, we confirmed that miR-155 inhibited the expression of C/EBPβ via binding sites in the 3'UTR of C/EBPβ mRNA. Both of C/EBPα and PPARγ, triggered by C/EBPβ, were also downregulated. In vivo, the expression of C/EBPβ, C/EBPα and PPARγ in mA-MSCs were suppressed due to uptake of exosomal miR-155. Thus, those findings proofed GC exosomal miR-155 impaired the adipogenesis of A-MSCs by inhibition of C/EBPβ.

In this study, we repoted that miR-155 was upregulated in both serum and A-MSCs of GC patients, attenuating adipo-differentiation of A-MSCs obtained from GC patients. In the meanwhile, we also found that GC exosomal miR-155 could be internalized into A-MSCs and inhibited adipogenetic progress of A-MSCs targeting C/EBPβ and inhibited C/EPBα and PPARγ. In animal model, knockdown of miR-155 in GC exosomes substantially reversed inhibited adipogenesis of A-MSCs. In conclusion, the present study contributes to understanding an significant role of miR-155 delivered by GC exosomes in regulating A-MSCs adipogenetic differention and illustrates new insights into therapeutic targets of cancer cachexia.

Abbreviations

MSCs: Mesenchymal stem cells; A-MSCs: Adipose-derived MSCs; mA-MSCs: MSCs from mice inguinal adipose tissues; GC: Gastric cancer; RT-PCR: Real time polymerase chain reaction; CAC: Cancer-associated cachexia; C/EBP: CCAAT/enhancer-binding protein; PPAR: preceding peroxisoe proliferator-activated receptor; FABPs; fatty acid-binding proteins; FATPs: fatty acid transport proteins

Declarations

Acknowledgements

The authors thank Meng Zhang, Jing Liu for their technical supports.

Authors' contributions

YL and DL contributed to performing the experiments, assembly of data and manuscript writing. HW, HZ, TD, RL, TN, and MB contributed to assembly of data. GY and YB contributed to the conception and design, revised and corrected the final manuscript.. All authors read and approved the final manuscript. performed the experiments.

Funding

This work was supported by grants from the National Natural Science Foundation of China (Nos. 81772629) and the Demonstrative Research Platform of Clinical Evaluation Technology for New Anticancer Drugs (No. 2018ZX09201015). This work was also supported by the Tianjin Science Foundation (Nos. 18JCQNJC81900) and the Science & Technology Development Fund of the Tianjin Education Commission for Higher Education (2018KJ046). The funders had no role in the study design,

the data collection and analysis, the interpretation of the data, the writing of the report, and the decision to submit this article for publication

Availability of data and materials

the datasets used and analyzed during the current study are also available from the corresponding author on reasonable request.

Ethics approval and consent to participate

The experiment on mice followed the internationally recognized guidelines. Meanwhile, ethical approval of animal research was signed and approved by approved by the Ethics Committee of Tianjin Medical University Cancer Institute and Hospital (approval no.Ek2019039).

Consent for publication

Not applicable.

Competing interests

The authors declare that they have no competing interests.

Author details

Tianjin Medical University Cancer Institute and Hospital, National Clinical Research Center for

Cancer, Tianjin's Clinical Research Center for Cancer, Key Laboratory of Cancer Prevention and

Therapy, Tianjin, 300060, China, Tianjin Medical University Cancer Institute and Hospital, Huan hu xi Road 18, Tianjin 300060 (China)

References

1. Baracos VE, Martin L, Korc M, Guttridge DC, Fearon KCH. Cancer-associated cachexia. Nature reviews Disease primers. 2018;4:17105.
2. Argilés JM, Stemmler B, López-Soriano FJ, Busquets S. Inter-tissue communication in cancer cachexia. Nature reviews Endocrinology. 2018;15(1):9–20.
3. Miller J, Dreczkowski G, Ramage MI, Wigmore SJ, Gallagher IJ, Skipworth RJE. **Adipose depot gene expression and intelectin-1 in the metabolic response to cancer and cachexia**. *Journal of cachexia, sarcopenia and muscle* 2020.
4. Rohm M, Schäfer M, Laurent V, Üstünel BE, Niopek K, Algire C, Hautzinger O, Sijmonsma TP, Zota A, Medrikova D, et al. An AMP-activated protein kinase-stabilizing peptide ameliorates adipose tissue wasting in cancer cachexia in mice. Nature medicine. 2016;22(10):1120–30.

5. Tang QQ, Lane MD. Adipogenesis: from stem cell to adipocyte. Annual review of biochemistry. 2012;81:715–36.
6. Guo L, Li X, Tang QQ. Transcriptional regulation of adipocyte differentiation: a central role for CCAAT/enhancer-binding protein (C/EBP) β. J Biol Chem. 2015;290(2):755–61.
7. Li Q, Gao Z, Chen Y, Guan MX. The role of mitochondria in osteogenic, adipogenic and chondrogenic differentiation of mesenchymal stem cells. Protein cell. 2017;8(6):439–45.
8. Hammarstedt A, Gogg S, Hedjazifar S, Nerstedt A, Smith U. Impaired Adipogenesis and Dysfunctional Adipose Tissue in Human Hypertrophic Obesity. Physiological reviews. 2018;98(4):1911–41.
9. Vishvanath L, Gupta RK. Contribution of adipogenesis to healthy adipose tissue expansion in obesity. J Clin Investig. 2019;129(10):4022–31.
10. Bougarne N, Weyers B, Desmet SJ, Deckers J, Ray DW, Staels B, De Bosscher K. Molecular Actions of PPARα in Lipid Metabolism and Inflammation. Endocr Rev. 2018;39(5):760–802.
11. Feng S, Reuss L, Wang Y. **Potential of Natural Products in the Inhibition of Adipogenesis through Regulation of PPARγ Expression and/or Its Transcriptional Activity**. *Molecules (Basel, Switzerland)* 2016, 21(10).
12. Walendzik K, Kopcewicz M, Bukowska J, Panasiewicz G, Szafranska B, Gawronska-Kozak B. The Transcription Factor FOXN1 Regulates Skin Adipogenesis and Affects Susceptibility to Diet-Induced Obesity. J Invest Dermatol. 2020;140(6):1166–75.e1169.
13. Kalluri R, LeBleu VS. **The biology, function, and biomedical applications of exosomes**. *Science (New York, NY)* 2020, 367(6478).
14. O'Brien K, Breyne K, Ughetto S, Laurent LC, Breakefield XO. **RNA delivery by extracellular vesicles in mammalian cells and its applications**. *Nature reviews Molecular cell biology* 2020:1–22.
15. Biswas AK, Acharyya S. Understanding cachexia in the context of metastatic progression. Nature reviews Cancer. 2020;20(5):274–84.
16. Cao Y, Sun Z, Liao L, Meng Y, Han Q, Zhao RC. Human adipose tissue-derived stem cells differentiate into endothelial cells in vitro and improve postnatal neovascularization in vivo. Biochem Biophys Res Commun. 2005;332(2):370–9.
17. Barton MK. Cancer cachexia awareness, diagnosis, and treatment are lacking among oncology providers. Cancer J Clin. 2017;67(2):91–2.
18. Sassoon DA. Fatty acid metabolism-the first trigger for cachexia? Nature medicine. 2016;22(6):584–5.
19. Ghaben AL, Scherer PE. Adipogenesis and metabolic health. Nature reviews Molecular cell biology. 2019;20(4):242–58.
20. Roeland EJ, Bohlke K, Baracos VE, Bruera E, Del Fabbro E, Dixon S, Fallon M, Herrstedt J, Lau H, Platek M, et al: **Management of Cancer Cachexia: ASCO Guideline**. *Journal of clinical oncology: official journal of the American Society of Clinical Oncology* 2020:Jco2000611.

21. Hu W, Ru Z, Zhou Y, Xiao W, Sun R, Zhang S, Gao Y, Li X, Zhang X, Yang H. Lung cancer-derived extracellular vesicles induced myotube atrophy and adipocyte lipolysis via the extracellular IL-6-mediated STAT3 pathway. Biochimica et biophysica acta Molecular cell biology of lipids. 2019;1864(8):1091–102.
22. Lima J, Simoes E, de Castro G, Morais M, de Matos-Neto EM, Alves MJ, Pinto NI, Figueredo RG, Zorn TMT, Felipe-Silva AS, et al. Tumour-derived transforming growth factor-β signalling contributes to fibrosis in patients with cancer cachexia. Journal of cachexia sarcopenia muscle. 2019;10(5):1045–59.
23. Zhang H, Zhu L, Bai M, Liu Y, Zhan Y, Deng T, Yang H, Sun W, Wang X, Zhu K, et al. Exosomal circRNA derived from gastric tumor promotes white adipose browning by targeting the miR-133/PRDM16 pathway. International journal of cancer. 2019;144(10):2501–15.
24. Gulei D, Raduly L, Broseghini E, Ferracin M, Berindan-Neagoe I. The extensive role of miR-155 in malignant and non-malignant diseases. Mol Aspects Med. 2019;70:33–56.
25. Zhou Z, Zhang H, Deng T, Ning T, Liu R, Liu D, Bai M, Ying G, Ba Y. Exosomes Carrying MicroRNA-155 Target Forkhead Box O3 of Endothelial Cells and Promote Angiogenesis in Gastric Cancer. Molecular therapy oncolytics. 2019;15:223–33.
26. Deng T, Zhang H, Yang H, Wang H, Bai M, Sun W, Wang X, Si Y, Ning T, Zhang L, et al. Exosome miR-155 Derived from Gastric Carcinoma Promotes Angiogenesis by Targeting the c-MYB/VEGF Axis of Endothelial Cells. Molecular therapy Nucleic acids. 2020;19:1449–59.
27. Watanabe Y, Watanabe K, Fujioka D, Nakamura K, Nakamura T, Uematsu M, Bachschmid MM, Matsui R, Kugiyama K. Protein S-glutathionylation stimulate adipogenesis by stabilizing C/EBPβ in 3T3L1 cells. FASEB journal: official publication of the Federation of American Societies for Experimental Biology. 2020;34(4):5827–37.
28. Millward CA, Heaney JD, Sinasac DS, Chu EC, Bederman IR, Gilge DA, Previs SF, Croniger CM. Mice with a deletion in the gene for CCAAT/enhancer-binding protein beta are protected against diet-induced obesity. Diabetes. 2007;56(1):161–7.
29. Han L, Wang B, Wang R, Gong S, Chen G, Xu W. The shift in the balance between osteoblastogenesis and adipogenesis of mesenchymal stem cells mediated by glucocorticoid receptor. Stem Cell Res Ther. 2019;10(1):377.
30. Lin Z, He H, Wang M, Liang J. MicroRNA-130a controls bone marrow mesenchymal stem cell differentiation towards the osteoblastic and adipogenic fate. Cell proliferation. 2019;52(6):e12688.
31. Cao Y, Gomes SA, Rangel EB, Paulino EC, Fonseca TL, Li J, Teixeira MB, Gouveia CH, Bianco AC, Kapiloff MS, et al. S-nitrosoglutathione reductase-dependent PPARγ denitrosylation participates in MSC-derived adipogenesis and osteogenesis. J Clin Investig. 2015;125(4):1679–91.

Figures

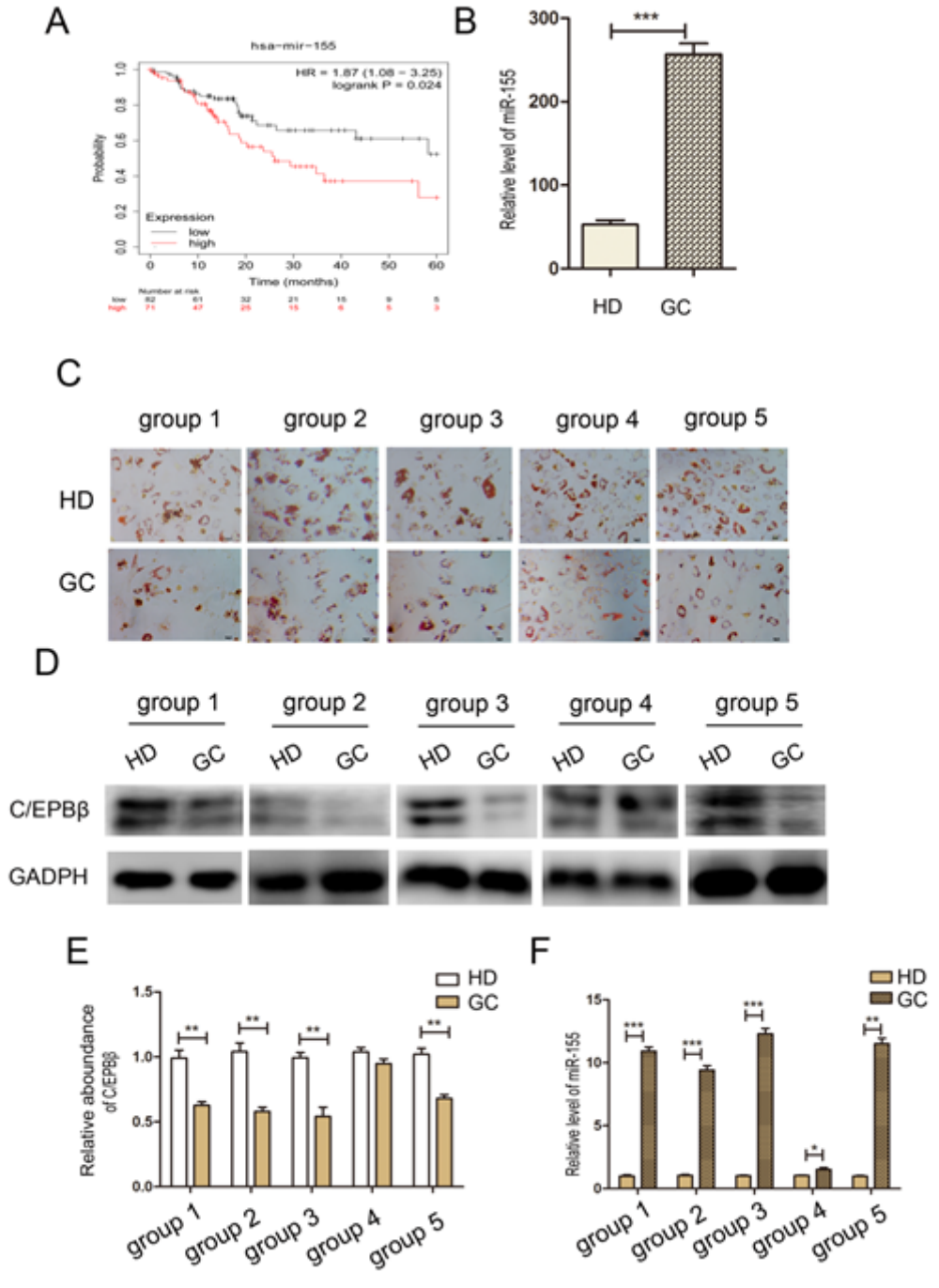

Figure 1

miR-155 shown negtive relationship with adipo-differentiation of A-MSC in GC patients (A) The relationship between miR-155 and the survival of GC from the tumor database (http://kmplot.com. n = in the miR-155-low group and n = in the miR-155-high group **p < 0.01). (B) Relative levels of miR-155 in GC serum and normal serum using RT-PCR (n=150). (C) Oil red O staining analysis of capacity of adipo-differentiation of A-MSC from GC patients and healthy donor (n=3). (D□E) Western blot analysis of C/EBPβexpression of A-MSC in GC patients (n=3). (F) Relative levels of miR-155 in A-MSC from GC patients and healthy donor (n=3).

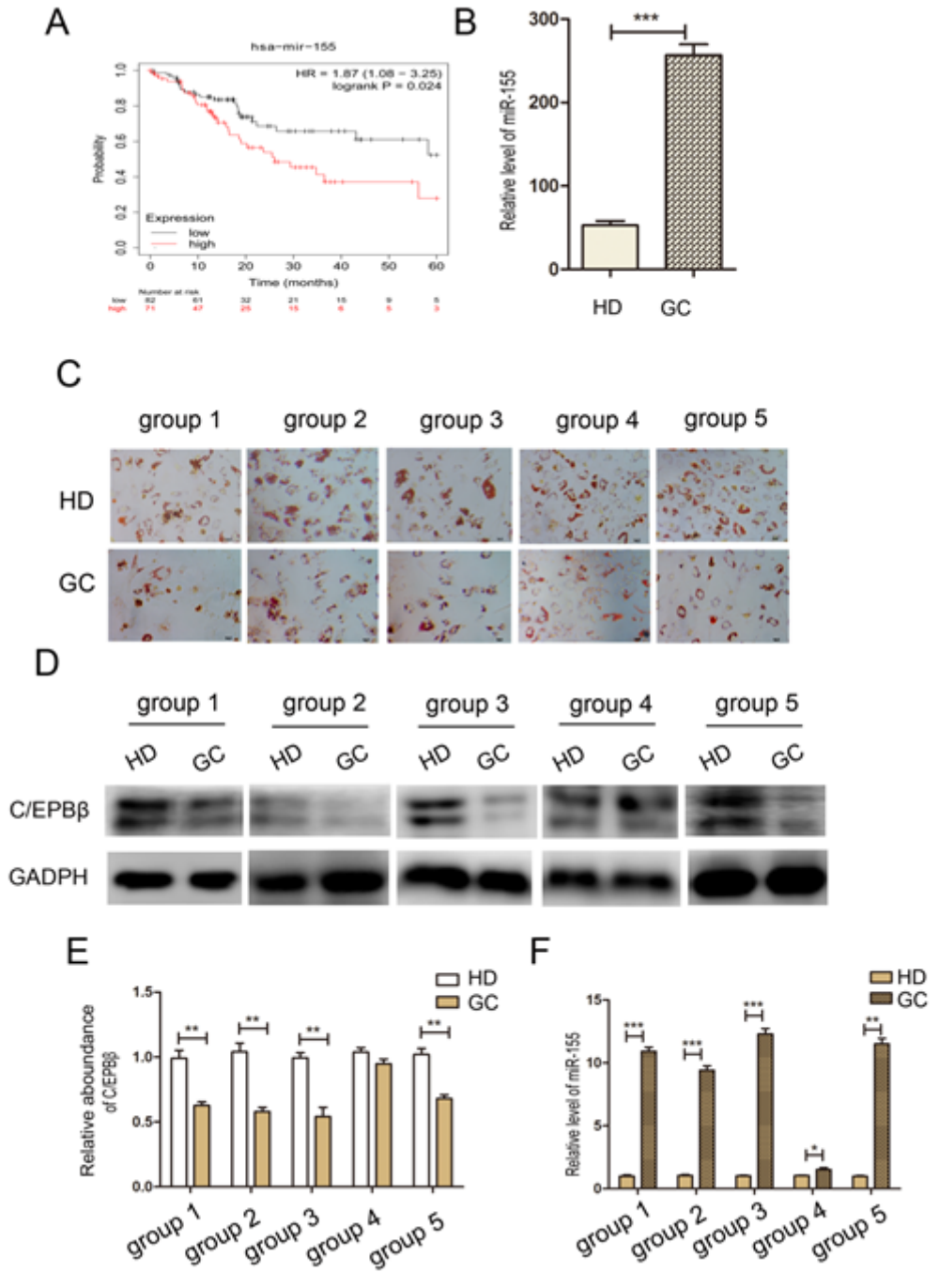

Figure 1

miR-155 shown negtive relationship with adipo-differentiation of A-MSC in GC patients (A) The relationship between miR-155 and the survival of GC from the tumor database (http://kmplot.com. n = in the miR-155-low group and n = in the miR-155-high group **p < 0.01). (B) Relative levels of miR-155 in GC serum and normal serum using RT-PCR (n=150). (C) Oil red O staining analysis of capacity of adipo-differentiation of A-MSC from GC patients and healthy donor (n=3). (D□E) Western blot analysis of C/EBPβexpression of A-MSC in GC patients (n=3). (F) Relative levels of miR-155 in A-MSC from GC patients and healthy donor (n=3).

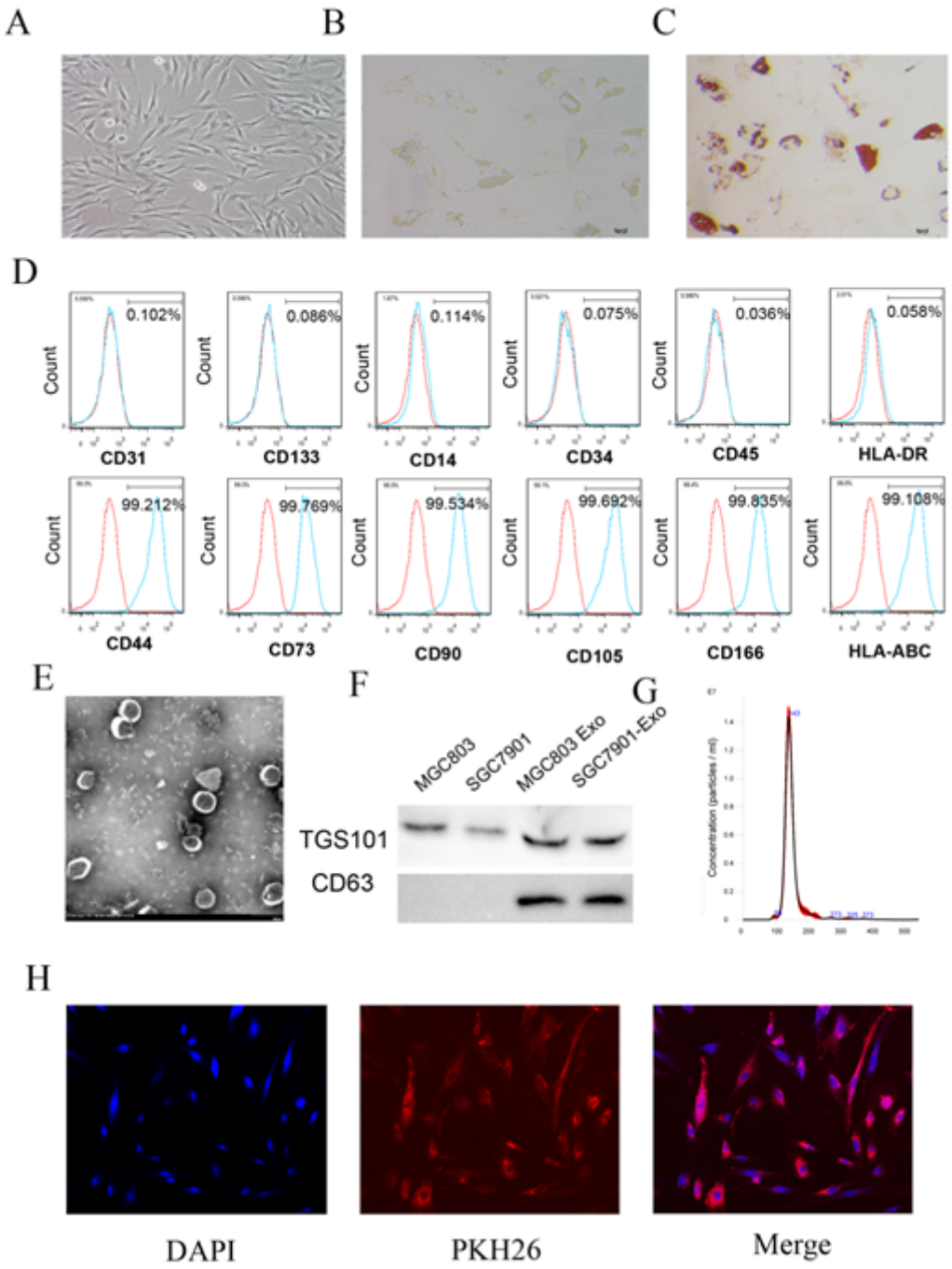

Figure 2

Identification and characterization of A-MSCs and GC exosomes (A) The morphology of A-MSCs. (B) The morphology of A-MSCs after adipo -differentiation. (C) Adipo-differentiation of A-MSCs stained by oil red O. (D) The immunophenotypic analysis of A-MSCs. (E) Representative transmission electron microscopy image of exosomes derived from GC cell (scale bar=500 nm). (F) Representative images of Tsg101 and CD63 expression, three exosomes-specific markers. (G) Nanoparticle tracking analysis (NTA) of SGC7901-exosomes. (H) PKH67-labeled SGC7901-exosomes can be taken up by A-MSCs.

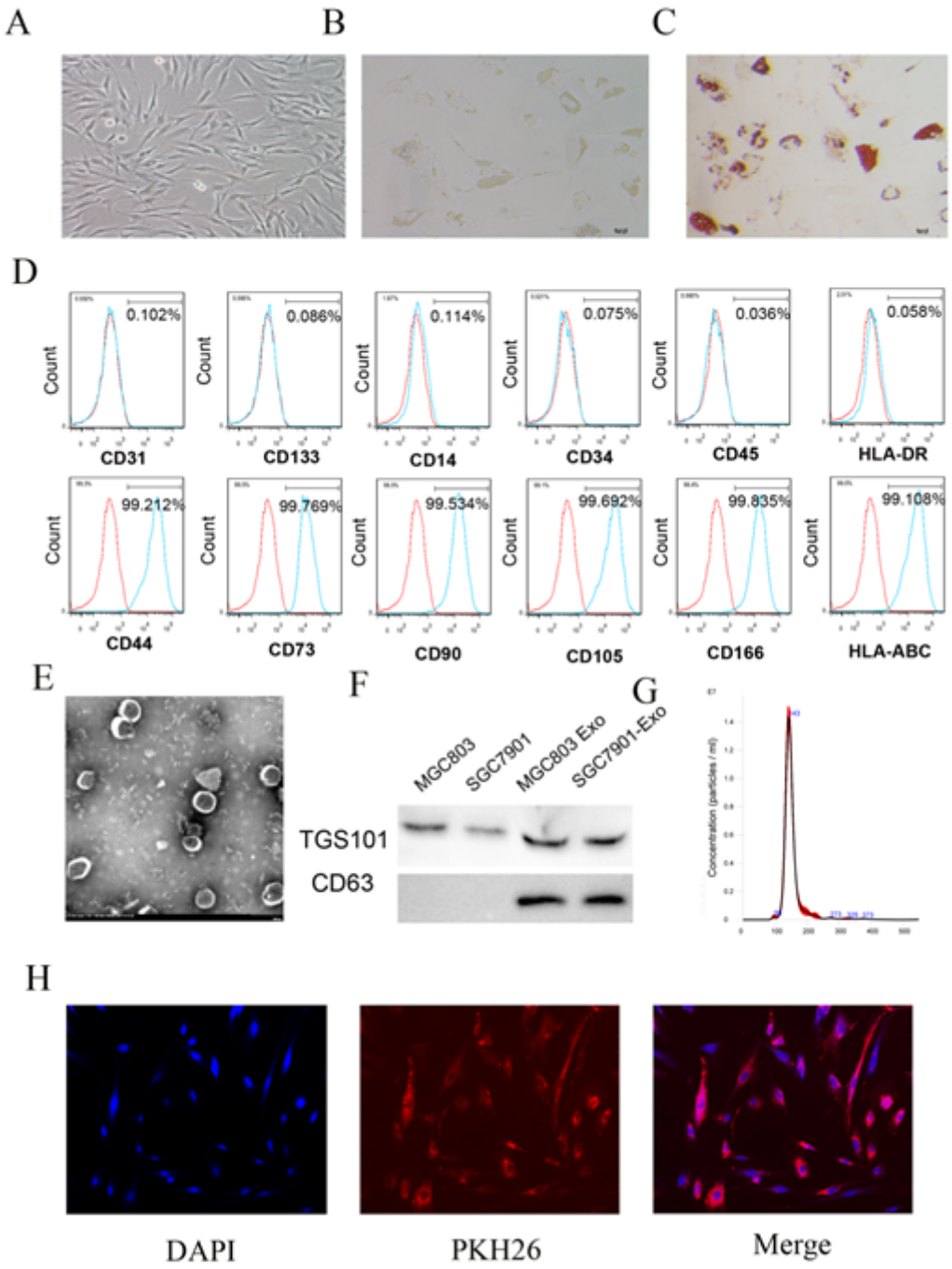

Figure 2

Identification and characterization of A-MSCs and GC exosomes (A) The morphology of A-MSCs. (B) The morphology of A-MSCs after adipo -differentiation. (C) Adipo-differentiation of A-MSCs stained by oil red O. (D) The immunophenotypic analysis of A-MSCs. (E) Representative transmission electron microscopy image of exosomes derived from GC cell (scale bar=500 nm). (F) Representative images of Tsg101 and CD63 expression, three exosomes-specific markers. (G) Nanoparticle tracking analysis (NTA) of SGC7901-exosomes. (H) PKH67-labeled SGC7901-exosomes can be taken up by A-MSCs.

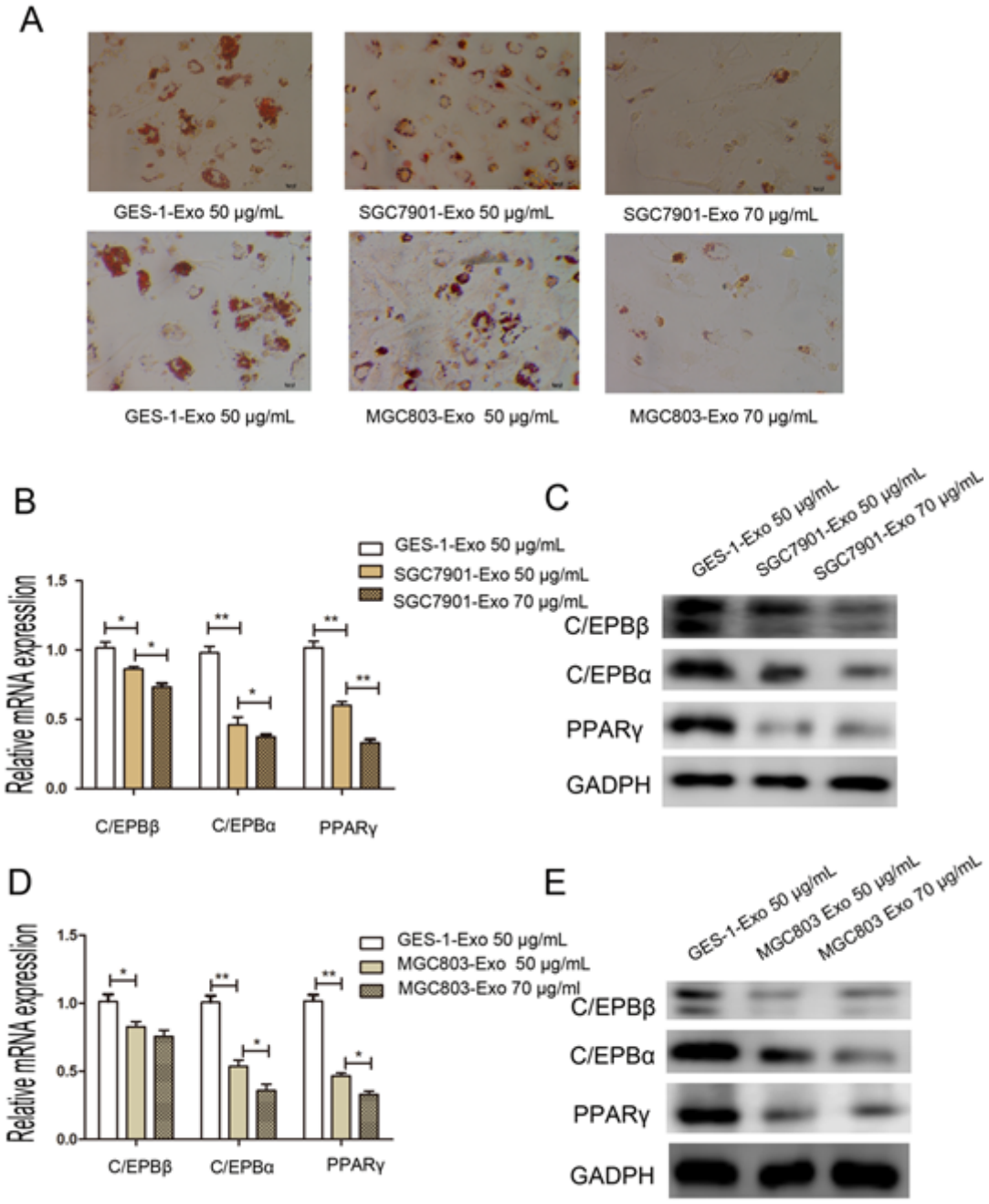

Figure 3

GC-exosomes inhibited adipo-differentiation of A-MSCs (A) Oil Red O staining was performed to visualize the lipid droplet accumulation in A-MSCs treated with GES-1 exosomes, SGC7901 exosomes or MGC803 exosomes. (B, D) RT-PCR analysis of adipogenic-specific genes (C/EBPβ, C/EBPα, PPARγ, normalized to GAPDH) in groups above. (C, E) Western blot analysis of C/EBPβ, C/EBPα, PPARγ in the groups above. *P\0.05, **P\0.01, ***P\0.001.

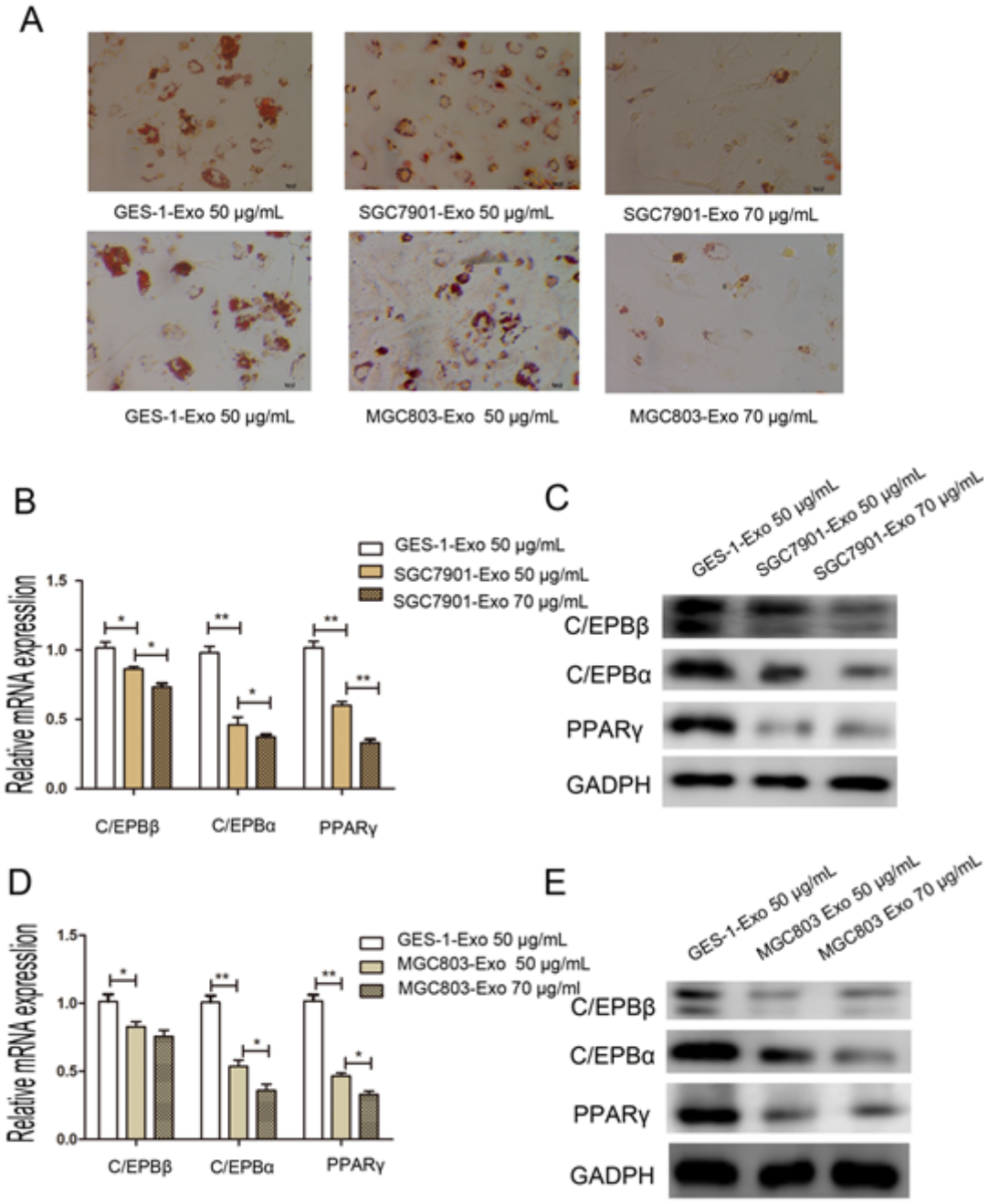

Figure 3

GC-exosomes inhibited adipo-differentiation of A-MSCs (A) Oil Red O staining was performed to visualize the lipid droplet accumulation in A-MSCs treated with GES-1 exosomes, SGC7901 exosomes or MGC803 exosomes. (B, D) RT-PCR analysis of adipogenic-specific genes (C/EBPβ, C/EBPα, PPARγ, normalized to GAPDH) in groups above. (C, E) Western blot analysis of C/EBPβ, C/EBPα, PPARγ in the groups above. *P\0.05, **P\0.01, ***P\0.001.

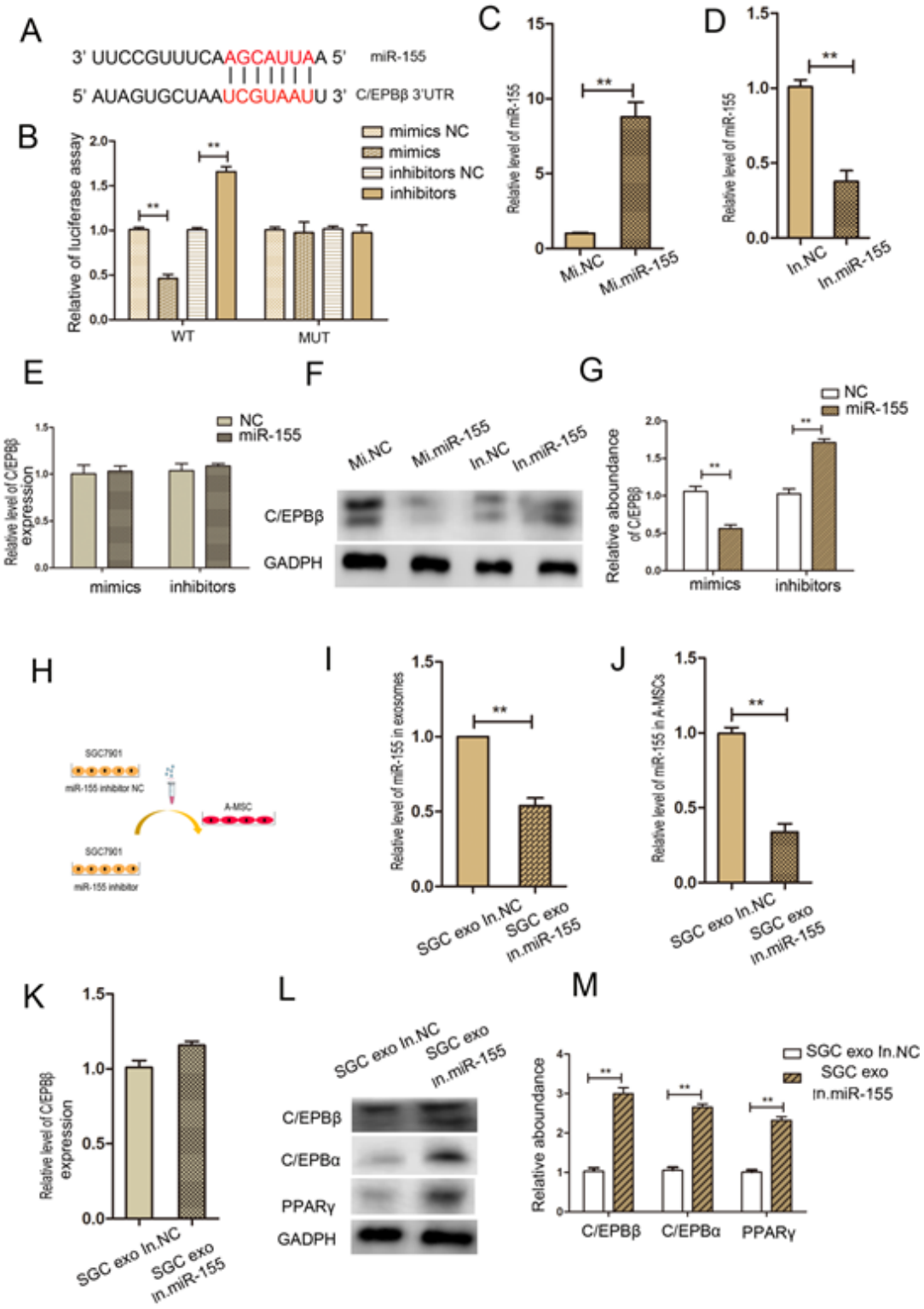

Figure 4

GC-exosomes-miR-155 targeting C/EBPβ in A-MSCs (A). The predicted binding sites for miR-155 in 3'UTR of C/EBPβ mRNA. (B). Direct recognition of C/EBPβ by miR-155 (n = 3). Fireflfly luciferase reporters containing either wild-type (WT) or mutant (Mut) C/EBPβ 3'UTR sequence, miR-155 mimics and the corresponding normal control were co-transfected into 293T cells. The relative luciferase levels were detected after transfection at 24h after transfection (n=3). (C-D) RT-PCR analysis of miR-155 levels in A-

MSCs transfected with miR-155 mimics and normal control (NC) mimics (n=3). (E) RT-PCR analysis of C/EBPβ mRNA level in the groups above (n=3). (F-G) C/EBPβ expression in A-MSCs treated with miR-155 mimics, normal control (NC) mimics, miR-155 inhibitors, normal control (NC) inhibitors (n=3). (H) Schematic description of the experimental design. Isolation of exosomes after inhibiting of miR-155 level in SGC7901 (exosomes-IN-miR-155) to add in A-MSCs. (I) RT-PCR assay of miR-155 level in exosomes-NC-miR-155, exosomes-IN-miR-155 (n=3) (J) RT-PCR assay of miR-155 level in A-MSCs treated with exosomes-NC-miR-155, exosomes-IN-miR-155 (n=3). (K) C/EBPβ mRNA levels in A-MSCs pretreated with different exosomes were detected by qRT-PCR (n = 3). (L-M) C/EBPβ, C/EBPα, PPARγ expression in A-MSCs treated with exosomes-NC-miR-155, exosomes-IN-miR-155 analysed by WB .*P\0.05, **P\0.01, ***P\0.001.

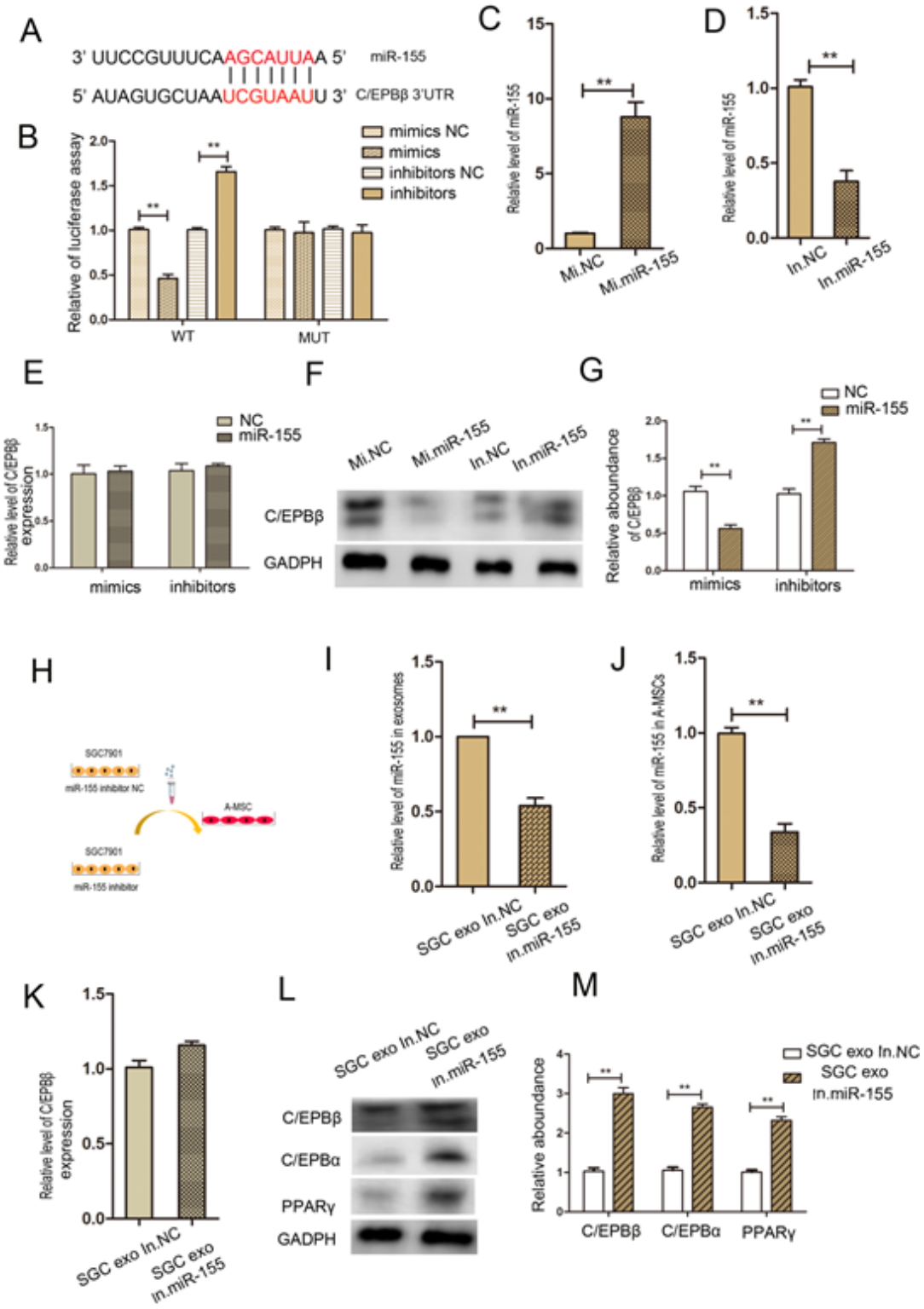

Figure 4

GC-exosomes-miR-155 targeting C/EBPβ in A-MSCs (A). The predicted binding sites for miR-155 in 3'UTR of C/EBPβ mRNA. (B). Direct recognition of C/EBPβ by miR-155 (n = 3). Fireflfly luciferase reporters containing either wild-type (WT) or mutant (Mut) C/EBPβ 3'UTR sequence, miR-155 mimics and the corresponding normal control were co-transfected into 293T cells. The relative luciferase levels were detected after transfection at 24h after transfection (n=3). (C-D) RT-PCR analysis of miR-155 levels in A-

MSCs transfected with miR-155 mimics and normal control (NC) mimics (n=3). (E) RT-PCR analysis of C/EBPβ mRNA level in the groups above (n=3). (F-G) C/EBPβ expression in A-MSCs treated with miR-155 mimics, normal control (NC) mimics, miR-155 inhibitors, normal control (NC) inhibitors (n=3). (H) Schematic description of the experimental design. Isolation of exosomes after inhibiting of miR-155 level in SGC7901 (exosomes-IN-miR-155) to add in A-MSCs. (I) RT-PCR assay of miR-155 level in exosomes-NC-miR-155, exosomes-IN-miR-155 (n=3) (J) RT-PCR assay of miR-155 level in A-MSCs treated with exosomes-NC-miR-155, exosomes-IN-miR-155 (n=3). (K) C/EBPβ mRNA levels in A-MSCs pretreated with different exosomes were detected by qRT-PCR (n = 3). (L-M) C/EBPβ, C/EBPα, PPARγ expression in A-MSCs treated with exosomes-NC-miR-155, exosomes-IN-miR-155 analysed by WB .*P\0.05, **P\0.01, ***P\0.001.

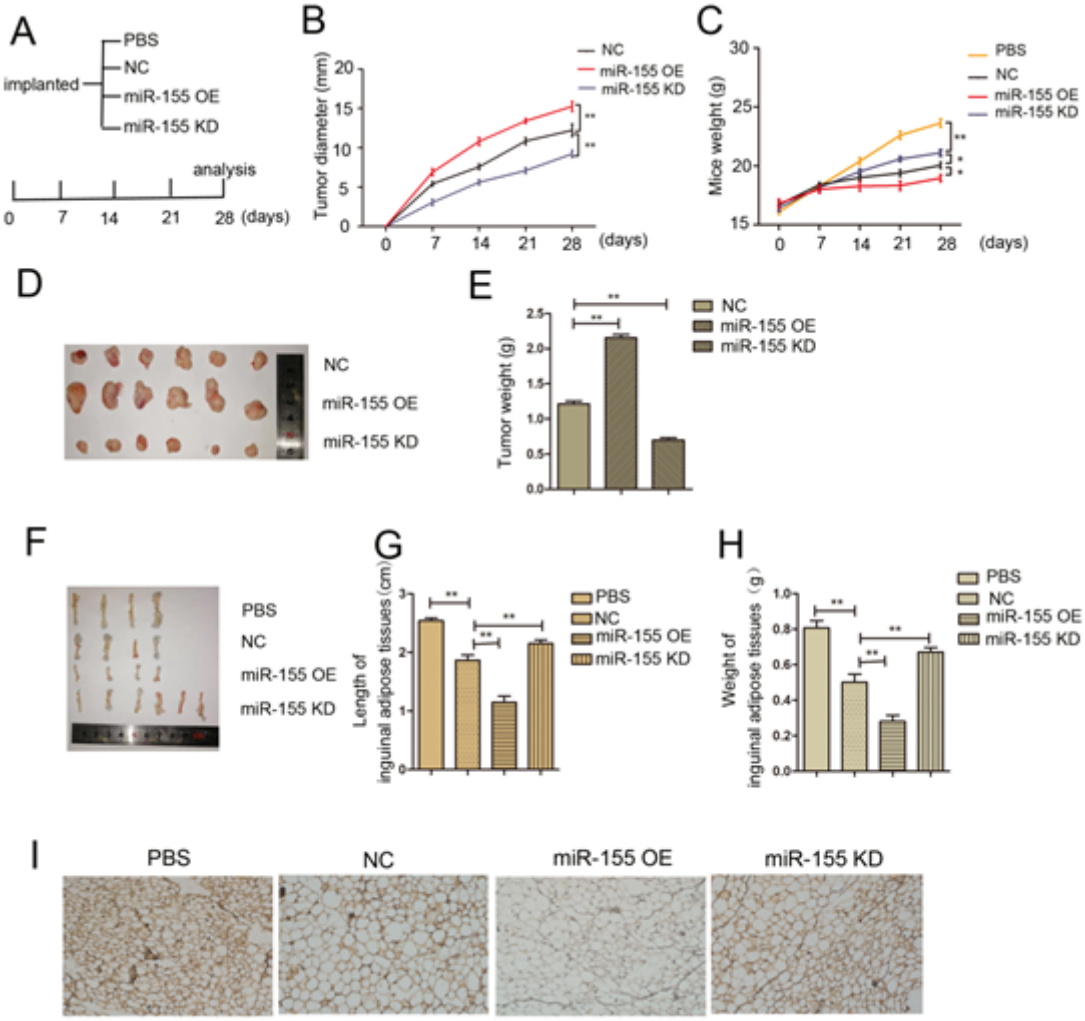

Figure 5

Influence of exosomessomal miR-155 in GC on loss of adipose tissue in vivo (A). A flow chart depicting the in vivo experimental design. (B) The diameter change of implanted tumor tissues. (C) The weight change of mice. (D-E) Representative Images of tumors in mice and analysis of the tumor weight. (F-H) Images of inguinal adipose tissue and analysis of the length and weight. (G) Images of paraffin-

embedded inguinal adipose tissue using FABP4 antibody by immunohistochemistry. *P\0.05, **P\0.01, ***P\0.001.

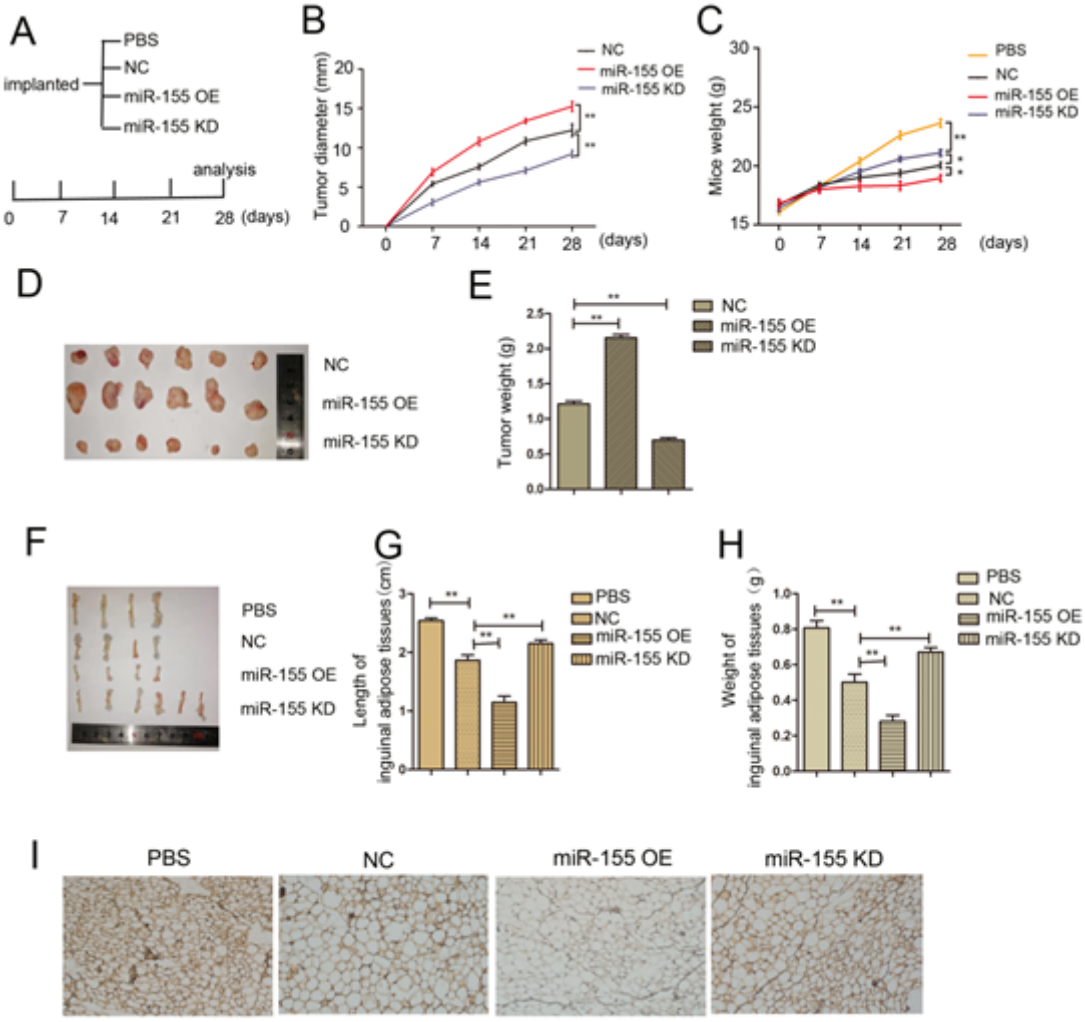

Figure 5

Influence of exosomessomal miR-155 in GC on loss of adipose tissue in vivo (A). A flow chart depicting the in vivo experimental design. (B) The diameter change of implanted tumor tissues. (C) The weight change of mice. (D-E) Representative Images of tumors in mice and analysis of the tumor weight. (F-H) Images of inguinal adipose tissue and analysis of the length and weight. (G) Images of paraffin-embedded inguinal adipose tissue using FABP4 antibody by immunohistochemistry. *P\0.05, **P\0.01, ***P\0.001.

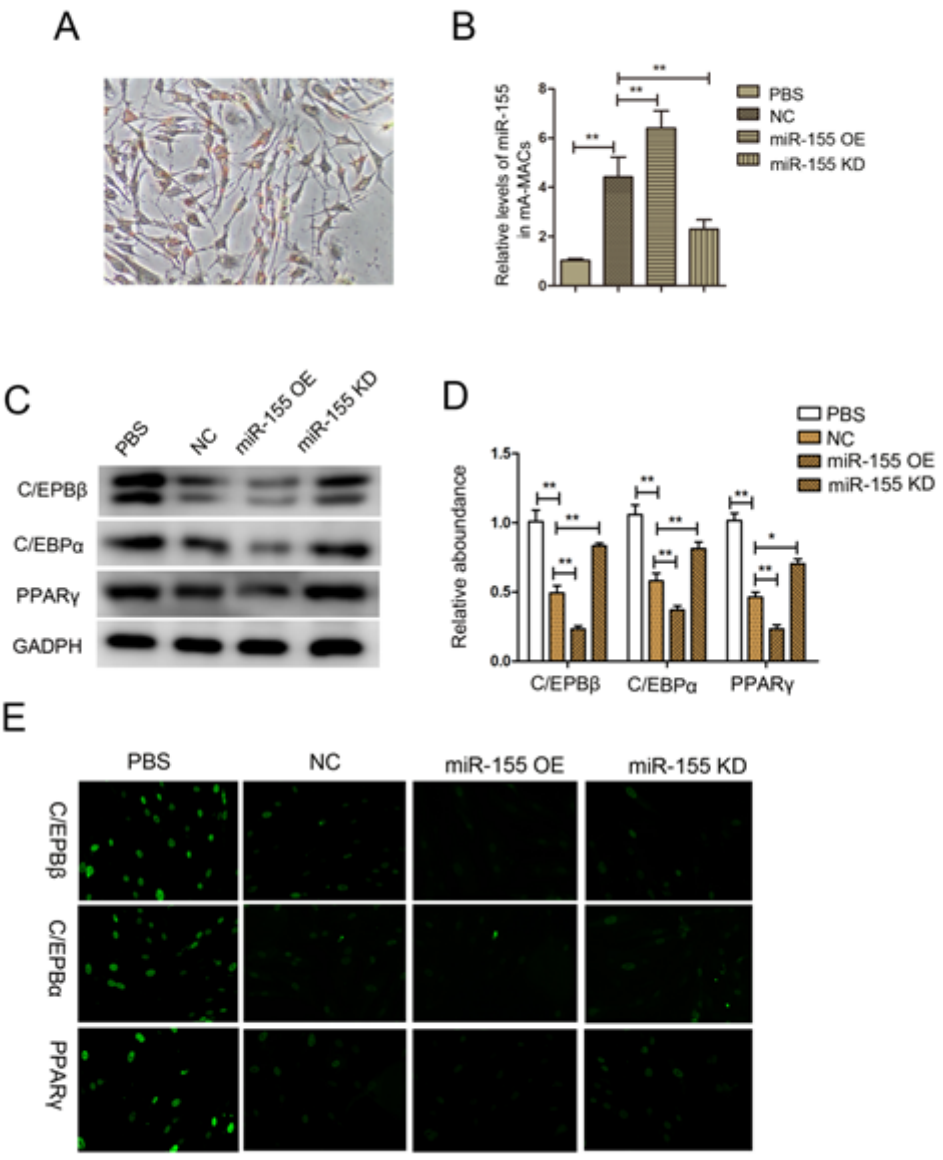

Figure 6

In vivo regulation of GC exosomes on adipo-differentiation in A-MSCs by miR-155/C/EBPβ axis (A) The morphology of mA-MSCs after adipo -differentiation. (B) Relative levels of miR-155 in mA-MSCs. (C-D) WB analysis of C/EBPβ, C/EBPα and PPARγ in mA-MSCs. (E) Immunoflfluorescence assay for C/EBPβ, PPARγ and C/EBPα (green labelling) which are markers of adipo-differentiation Scale bar = 50 μm. ** indicates p< 0.01 and *** indicates p< 0.001.

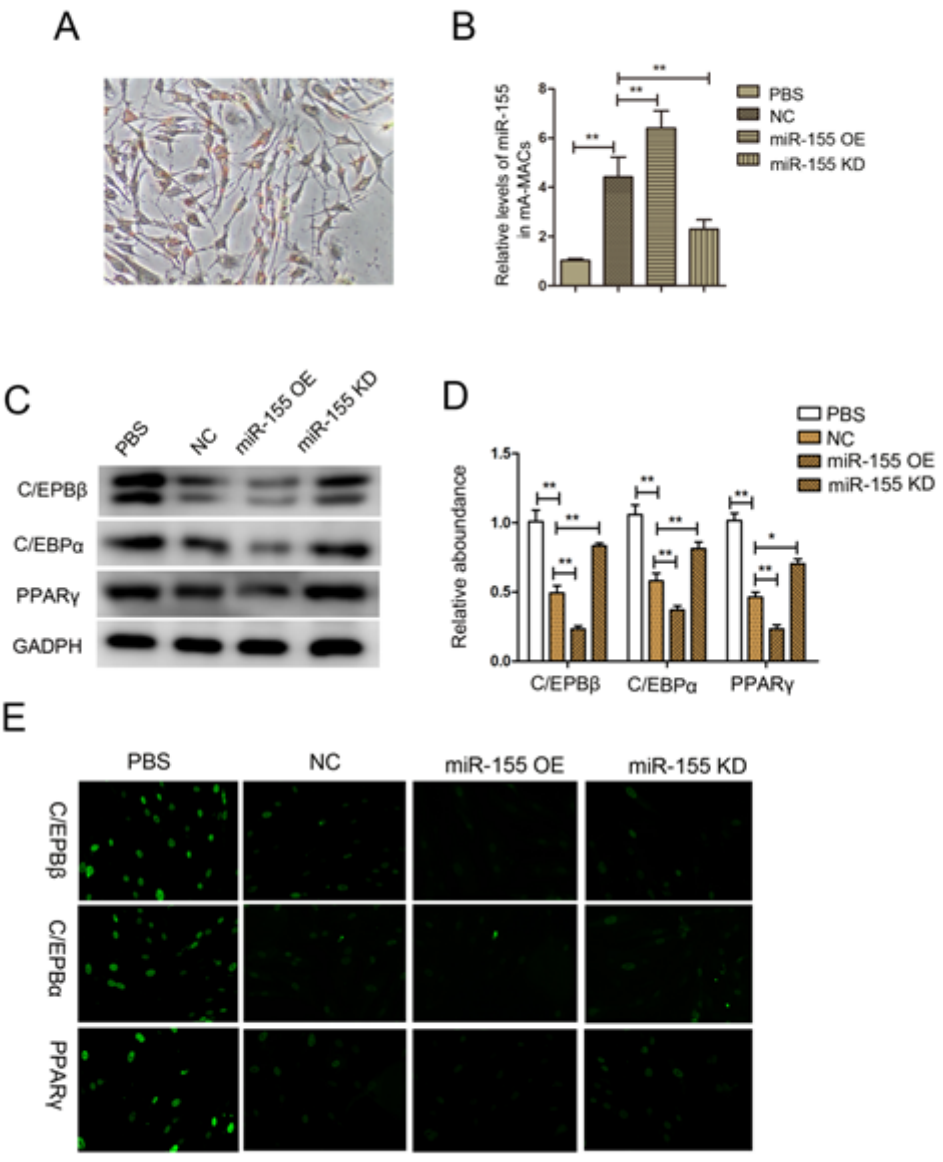

Figure 6

In vivo regulation of GC exosomes on adipo-differentiation in A-MSCs by miR-155/C/EBPβ axis (A) The morphology of mA-MSCs after adipo -differentiation. (B) Relative levels of miR-155 in mA-MSCs. (C-D) WB analysis of C/EBPβ, C/EBPα and PPARγ in mA-MSCs. (E) Immunoflfluorescence assay for C/EBPβ, PPARγ and C/EBPα (green labelling) which are markers of adipo-differentiation Scale bar = 50 μm. ** indicates p< 0.01 and *** indicates p< 0.001.

Supplementary Files

This is a list of supplementary files associated with this preprint. Click to download.

- supplymentalinformation.docx

- supplymentalinformation.docx